

# **High-impedance Transition-Edge-Sensors for wide field of view X-ray spectro-imagers and development of the associated cryogenic electronics and microelectronics**

**GDR DéTECTEURS et INSTRUMENTATIONS pour les 2 Infinis,  
IP2I, Lyon, 18-20 juin 2025**

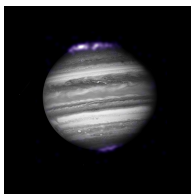
Benjamin Criton

CEA/IRFU/DEDIP/LISETA & DAp  
*benjamin.criton@cea.fr*

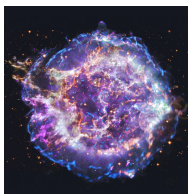
# Astrophysical background

Why do we require high spectral and spatial resolution images of spatially spread X-ray emitting astrophysical objects?

- Numerous (nearly all) astrophysical objects emit in the soft X-ray band (100 eV to 10 keV).
- X-ray emissions come from heated gases (1-100 MK) or Bremsstrahlung, cyclotron.
- Emissions encountered in many parts of the universe:



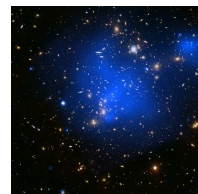
Jupiter and its two X-ray emitting aurorae



Cassiopeia A supernovae (Si, S, Ca, Fe)



NGC1672 (Chandra, composite)



Abell 2744, X-ray emitting galaxy cluster (Chandra, composite)

Need for high spectral resolution in hot plasmas:  $10\text{-}100 \text{ km/s } \mathcal{O} \text{ eV}$ .

# Micro-calorimeters

How to achieve high resolution X-ray spectro-imaging of spatially spread astrophysical objects ?

→ **X-ray micro-calorimeters: far better spectral resolution than CCD: 2 eV and array fabrication possible.**

- Image = photon flux on each pixel .
- Energy spectrum = energy of each photon, measured and stored.
- Spectro-image = cube of data.

Working principle : we measure the temperature rise produced by the absorption of an X-ray photon in the absorber using a very sensitive thermometer.

$$\Delta T = \frac{\Delta E}{C}, \langle \Delta E^2 \rangle = k_B T^2 C \text{ and } dV/dT = I \frac{dR}{dT} \quad (1)$$

⇒ Two main optimisation paths for spectral resolution: ↘ **heat capacity C** & ↗ **sensor sensitivity dR/dT**.

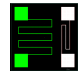
→ Two main types of thermometers: Doped Silicon thermistors and superconducting TES (+KIDs, MMC, ...).

→ Main  $\mu$ -calorimeter's constraint: **works around 100 mK** ⇒ strong constraints in satellites refrigerators.

# Reduction of the electron-phonon decoupling in HRTEs



Goal: reduce the e-ph decoupling to preserve the signal's amplitude.  
 ⇒ Solution: the active electro-thermal feedback.



## Classical method:

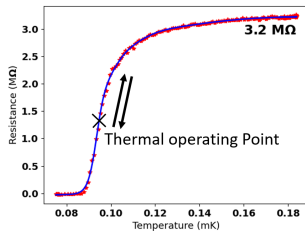
- Thermometer voltage biasing
- $P_J$  in **thermometer** ↘ when  $T \nearrow$
- Passive thermal feedback
- Advantage :

  - Simplicity.

- Disadvantages :

  - Strong biasing current.
  - High electron-phonon decoupling.
  - Sensitivity loss.

$$P_J = \frac{U^2}{R} = RI^2$$



## Innovative method:

- Thermometer current biasing
- $P_J$  in **heater** ↘ when  $T \nearrow$
- Active electro-thermal feedback
- Advantages:

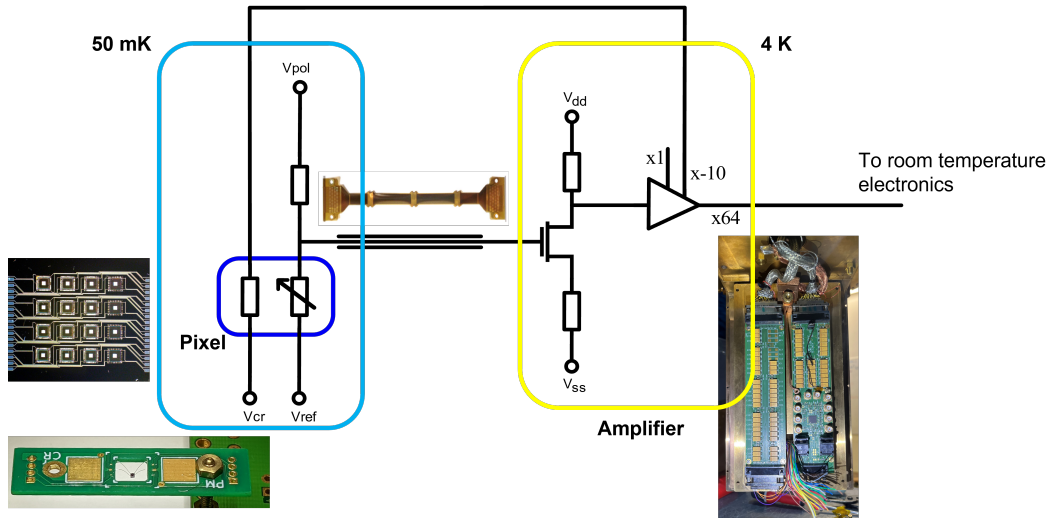
  - Low electron-phonon decoupling.
  - Increased sensitivity.

- Disadvantages :

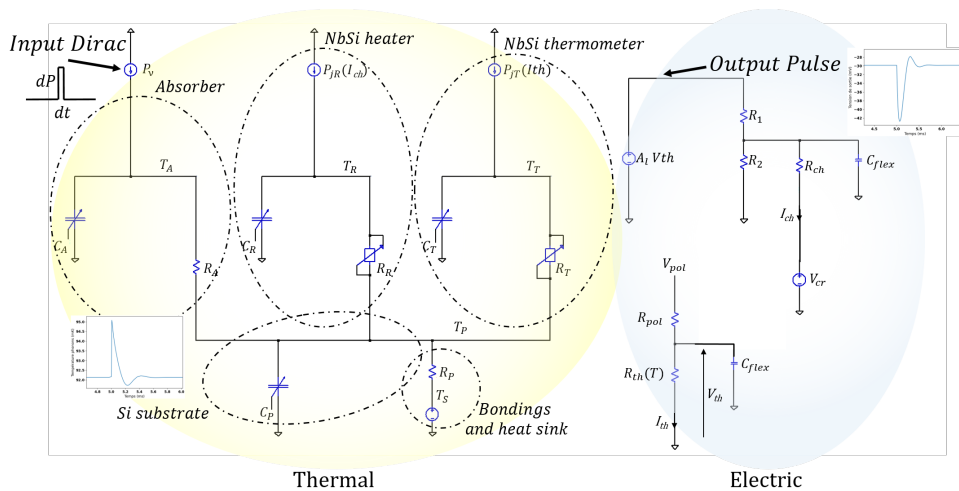
  - Amplifier feedback signal.
  - 2 signals instead of 1 to multiplex.

# System modelling and optimisations

# System overview

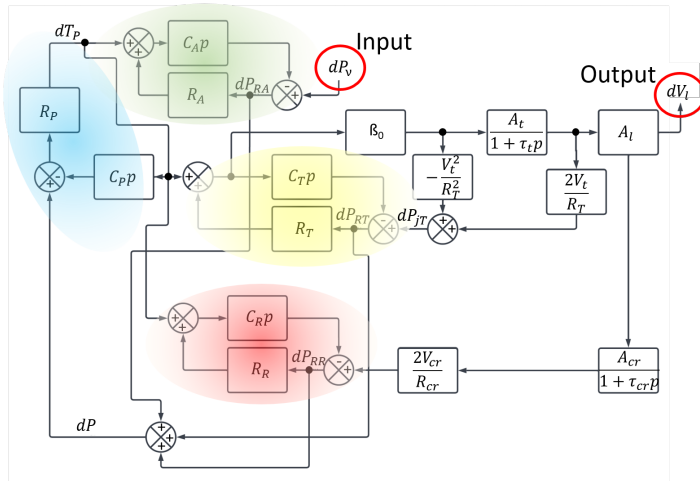


# System modelling



Electro-thermal model  $\implies$  operating point, time response, saturations, instabilities.  
**Non-linear model.**

# System modelling: linearisation and block diagram



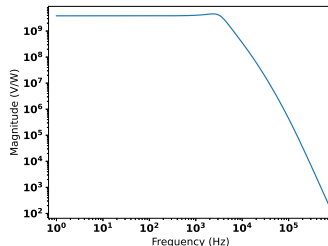
Small signal model  $\implies$  Frequency response, noise spectrum analysis.

# Small signal model and frequency response

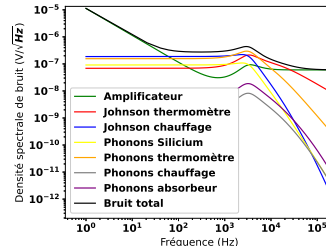
- Frequency response computation
- Noise spectral density computation

⇒ Spectral resolution calculation assuming optimal filtering:

$$\Delta E_{FWHM} = \frac{1}{q} \frac{2\sqrt{2\ln(2)}}{\sqrt{\int_0^{\infty} \frac{4}{NEP(f)^2} df}} \text{ [eV], NEP}(f) = 1/RSB(f). \quad (2)$$

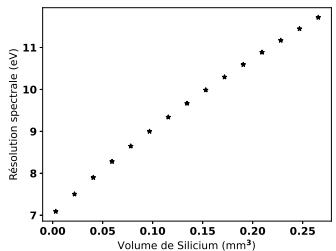


Frequency response of the system.

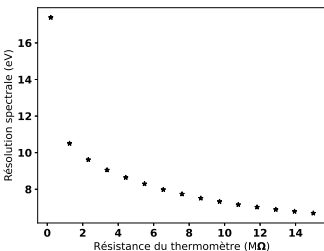


Noise power spectral density of the system.

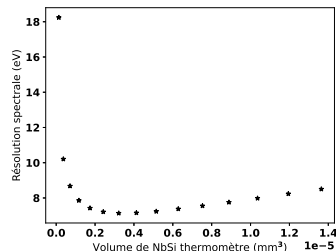
# Evolution of the spectral resolution for some parameters



Spectral resolution as a function of Si volume.



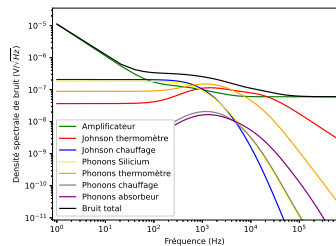
Spectral resolution as a function of normal state NbSi resistance.



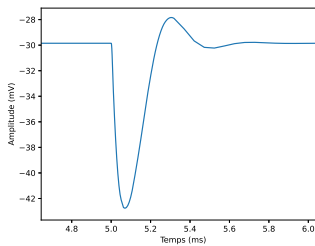
Spectral resolution as a function of NbSi volume (constant resistance).

# Optimisation of the detector's spectral resolution

2.1 eV spectral resolution in simulation on an optimised pixel. Comparable with best low impedance TESs.



Noise power spectrum of the optimised pixel. RMS noise:  $37 \mu\text{V}$  (100 Hz-100 kHz).

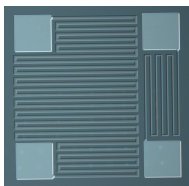


Impulse response from a 1 keV photon (Spice using optimal parameters). Amplitude:  $\sim 12 \text{ mV}$ .

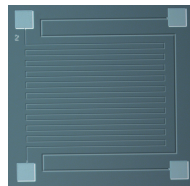
# Experimental measurements on pixels

# Fabrication of a batch of suspended pixels

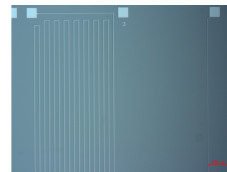
- Three Si volumes: 2-by-2 mm, 1-by-1 mm and 0.5-by-0.5 mm.
- Different NbSi TES and heater volumes and resistances.
- Layout design and fabrication by Stefanos Marnieros and Christine Oriol (IJCLab)!



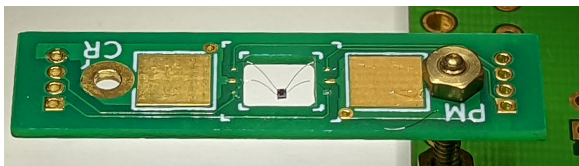
Microscope image of a 0.5 mm side width, 7  $\mu\text{m}$ , 8.7 mm NbSi meander pixel.



Microscope image of a 1 mm side width, 3  $\mu\text{m}$ , 16 mm NbSi meander pixel.

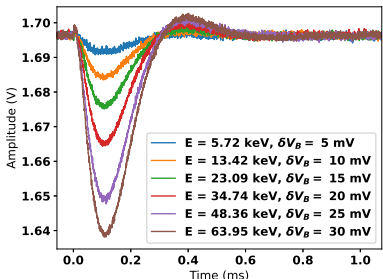


Microscope image of a 2 mm side width, 7  $\mu\text{m}$ , 31.3 mm NbSi meander pixel.

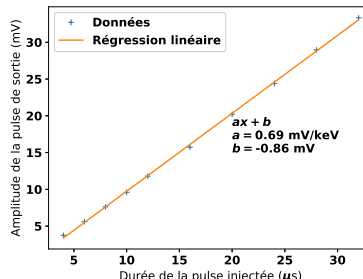


# Study of a suspended 2 mm pixel (old batch)

- Electric pulse injection using the on-chip heater on a “heavy” pixel.
- Inject heat pulses of different energies  $\Rightarrow$  **on-chip calibration tool**.
- Estimation of the Amplitude/Energy gain.



Output pulses for different heater-injected energies.

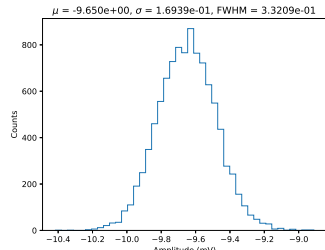


Output amplitude vs input pulse (Dirac) duration.

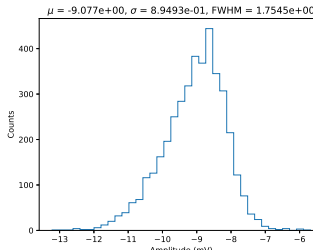
Conclusion: energy/amplitude gain:  $0.69 \text{ mV/keV}$ , low. High linearity. Gain differs from simulation: **Si volume, electronic heat capacity and heat conduction to sink suspected**.

# Amplitude spectra on a 2 mm pixel

- Measurements on a “heavy” 2 mm pixel with **2.4 nA biasing**.
- Better energy resolution with heater-injected pulses compared to Iron 55.



Amplitude spectrum for heater-injected  $\sim 14$  keV pulses.  $\Delta E_{FWHM} = 500$  eV.  
Biasing current: 2.4 nA.



Amplitude spectrum from  $^{55}\text{Fe}$  X-ray photons.  $\Delta E_{FWHM} = 1073$  eV. Biasing current: 2.4 nA.

Conclusion: coarse spectral resolution: 500 eV at 14 keV and 1000 eV for  $^{55}\text{Fe}$  X-ray. A lot is due to **very high and variable low frequency noise**.  $\Rightarrow$  design of an improved set-up.

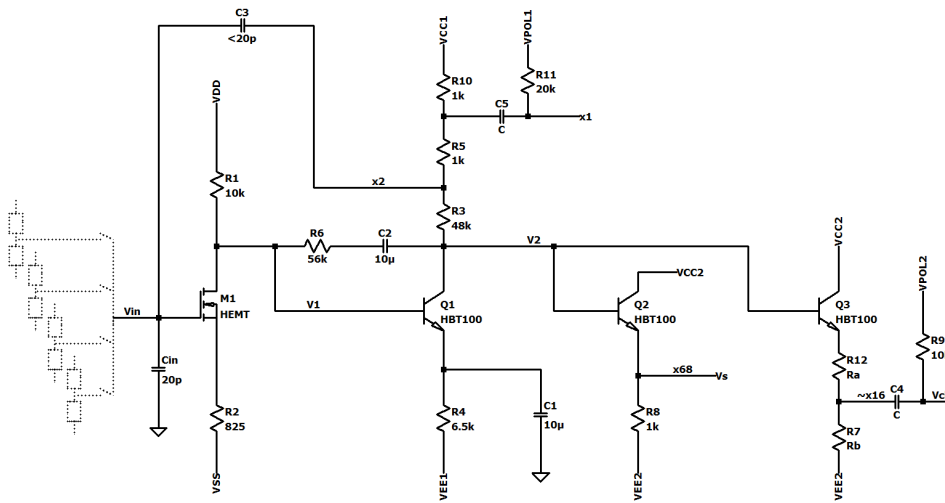
# Design of a low noise 4 K HEMT-SiGe amplifier

# Requirements for a new low-noise cryo-amplifier

Requirement: Design a 4 K amplifier having low input voltage noise (around  $1 \text{ nV}/\sqrt{\text{Hz}}$ ), high input impedance and low impedance outputs.

- High impedance input transistor.
  - MOS transistors too noisy at 4 K in our bandwidth (100 Hz-100 kHz).
  - SiGe HBT very interesting: high  $\beta \sim 1000$ , low noise  $\sim 0.37 \text{ nV}/\sqrt{\text{Hz}}$  but  $6 \text{ k}\Omega$  input impedance.  
⇒ CryoHEMT (Yong Jin C2N): high input impedance, low noise ( $\sim 0.3 \text{ nV}/\sqrt{\text{Hz}}$  @ 1 kHz).
- Low input capacitance: no Miller effect on first stage.
- Gain stability between cool-downs and during long runs.
- $\sim 10 \text{ mV}$  input dynamic range with gain 64.
- $< 1 \text{ k}\Omega$  output impedance for room temperature signal.
- DC coupling: information on the TES biasing.
- HEMT only for first stage.

# Schematic of the 4 K HEMT-SiGe amplifier board



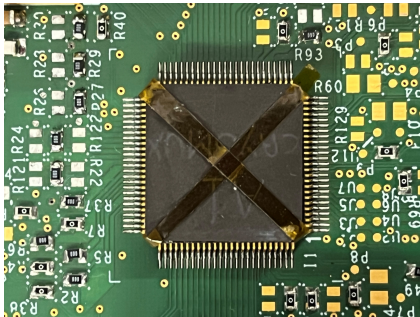
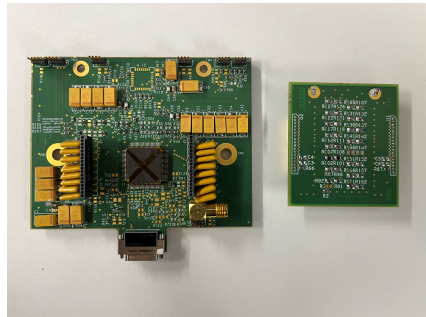
Design of the 16-to-1 50 mK high-impedance  
multiplexing ASIC

# Some figures

- Sampling frequency:
  - 16 pixels to multiplex, 10 samples per pulses ( $500 \mu\text{s}$  pulses).  
⇒ Multiplexing cycle  $< 50 \mu\text{s}$ .  
⇒ Sampling time  $< 3.125 \mu\text{s}$ 
    - We choose a  **$3 \mu\text{s}$  sampling time** and a  $48 \mu\text{s}$  multiplexing time.
- Coping with the input capacitance:
  - Around 50 pF measured.
  - ex.: 20 pF and  $1 \text{ M}\Omega$  detector:  $\tau = 20 \mu\text{s}$ , 7x higher than sampling time ( $3 \mu\text{s}$ ).
    - ex.: for a 95% value after a  $1 \mu\text{s}$  readout, the input capacitance should be 0.3 pF.  
⇒ physically impossible ⇒ **need for capacity compensation**.
- Maintaining the heater feedback voltage:
  - Need for 1.6 nF for a voltage drop  $< 0.1 \text{ mV}$  with a heater biasing at 10 mV.  
⇒ Large value integrated capacitors ⇒ **integrated NMOS capacitor**.

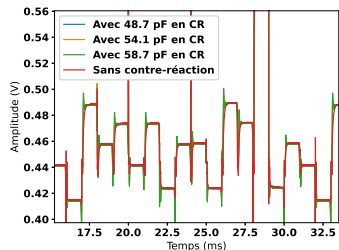
# Experimental measurements

- Functional tests from room temperature to  $\sim 150$  mK.
- Noise level below  $40 \text{ nV}/\sqrt{\text{Hz}}$  at room temperature.
- Operating at 30 mK since 2022.

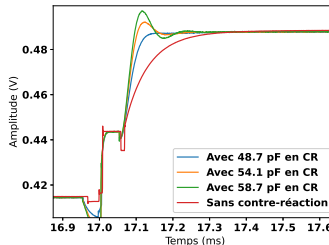


# Room temperature tests of the feedback capacitor.

We want to evaluate the effect of the feedback capacitor to compensate for the input capacitance



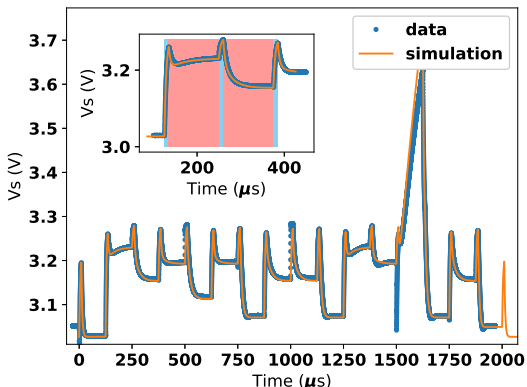
Multiplexing of 16 resistors ranging from  $110\text{ k}\Omega$  to  $1.1\text{ M}\Omega$ . 1 ms per resistor.



Multiplexing of 16 resistors ranging from  $110\text{ k}\Omega$  to  $1.1\text{ M}\Omega$ . Zoom on the readout of the  $1\text{ M}\Omega$  resistor.

Conclusion: the feedback capacitor increases the speed but creates instability at room temperature due to the flex series resistance when loading the reset voltage.

## 50 mK multiplexing.



50 mK multiplexing of resistors from 0  $\Omega$  to 1  $M\Omega$ . 125  $\mu s$  per pixel.

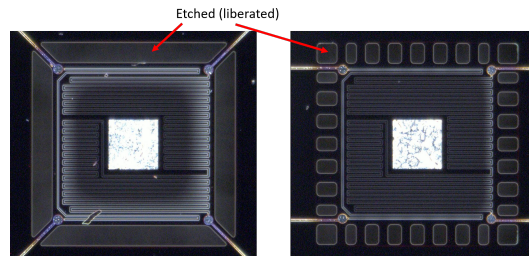
Conclusion: multiplexing at temperatures below 1 K is functional. Noise spectra show EM pickup around 1 kHz.

# Design and fabrication of the 4-by-4 NbSi matrices

# Matrices design

Matrix fabrication validates the feasibility of NbSi arrays for X-ray spectro-imaging.

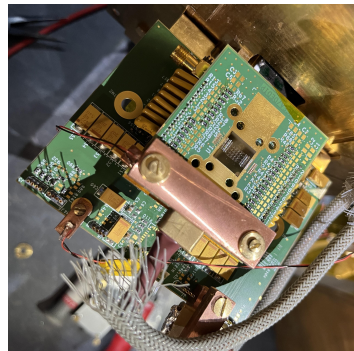
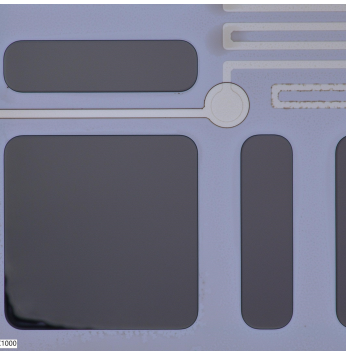
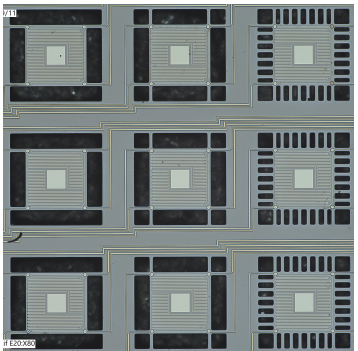
- Pixels multiplexed with the 50 mK ASIC.
  - 25 matrices on a wafer.
  - Each matrix has different pixel properties.
- ⇒ **Many physical parameters explored in one run.**
- Si bridges heat conduction at 100 mK:
    - bridge lengths : 60  $\mu\text{m}$  or 120  $\mu\text{m}$ .
    - bridge widths : 10  $\mu\text{m}$  or 30  $\mu\text{m}$ .
    - bridge nb. and orientations: 4, 8 and 32.
  - Different TES meanders: evaluate decoupling, limiting current, transitions and specific heat.



Layout and fabrication: S. Marnieros, L. Bergé at IJCLab & C2N!

## Fabrication results

- High fabrication yield.
- Some scratches after DRIE.
- Wafer thermalised using 30  $\mu\text{m}$  of Silver-filled epoxy.



Conclusion: array fabrication achieved. Normal resistance  $\sim 2.6 \text{ M}\Omega$ . No superconducting transition observed: NbSi evaporation issue?

# Conclusion

# Conclusion

**Realise a small-size demonstrator of a soft X-ray spectro-imaging chain to explore high resistivity TESs as an alternative to regular TESs**

- ✓ Evaluate theoretical potential of this technology.
- ✓ Realistic optimisation leading to 2.1 eV resolution for 500  $\mu\text{m}$  pixels. (TBC with measurements)
- ✓ Simplified single pixels designed and measured.
- ✓ Proved correct functioning of the system and shown detection of X-ray photons.
- ✓ New developments in cryogenic electronics.
- ✓ Operating 50 mK CMOS multiplexing ASIC.
- ✓ High yield fabrication of 16 pixels NbSi matrices on SOI.

# Annexes

# Optimal filtering and small signal model

Goal : confirm by simulation the correct functioning of two **experimental** “optimal” filters for spectral resolution estimations and verify they retrieve the expected theoretical best resolution.

- We know the theoretical spectral resolution of a test pixel

# Optimal filtering and small signal model

Goal : confirm by simulation the correct functioning of two **experimental** “optimal” filters for spectral resolution estimations and verify they retrieve the expected theoretical best resolution.

- We know the theoretical spectral resolution of a test pixel
  - We simulate a set of noisy pulses (400-500):
    - A time domain pulse is obtain by simplifying the transfer function.
    - We generate a set of identical pulses.
    - Independent noise with given PSD added to the pulses.
- ⇒ A set of independent noisy pulses is obtained.

# Optimal filtering and small signal model

Goal : confirm by simulation the correct functioning of two **experimental** “optimal” filters for spectral resolution estimations and verify they retrieve the expected theoretical best resolution.

- We know the theoretical spectral resolution of a test pixel
- We simulate a set of noisy pulses (400-500):
  - A time domain pulse is obtain by simplifying the transfer function.
  - We generate a set of identical pulses.
  - Independent noise with given PSD added to the pulses.

⇒ A set of independent noisy pulses is obtained.
- Two optimal filters under study:
  - Wiener deconvolution (frequency domain filtering).
  - Curve fitting (time domain filtering).

# Optimal filtering and small signal model

Goal : confirm by simulation the correct functioning of two **experimental** “optimal” filters for spectral resolution estimations and verify they retrieve the expected theoretical best resolution.

- We know the theoretical spectral resolution of a test pixel
- We simulate a set of noisy pulses (400-500):
  - A time domain pulse is obtain by simplifying the transfer function.
  - We generate a set of identical pulses.
  - Independent noise with given PSD added to the pulses.

⇒ A set of independent noisy pulses is obtained.
- Two optimal filters under study:
  - Wiener deconvolution (frequency domain filtering).
  - Curve fitting (time domain filtering).
- Spectral resolution estimation with these two methods.

# Optimal filtering and small signal model

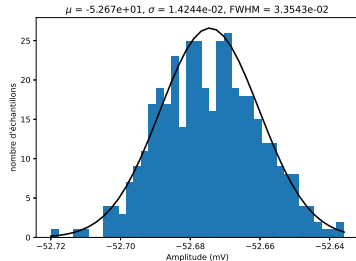
Goal : confirm by simulation the correct functioning of two **experimental** “optimal” filters for spectral resolution estimations and verify they retrieve the expected theoretical best resolution.

- We know the theoretical spectral resolution of a test pixel
- We simulate a set of noisy pulses (400-500):
  - A time domain pulse is obtain by simplifying the transfer function.
  - We generate a set of identical pulses.
  - Independent noise with given PSD added to the pulses.

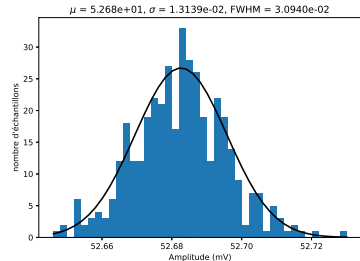
⇒ A set of independent noisy pulses is obtained.
- Two optimal filters under study:
  - Wiener deconvolution (frequency domain filtering).
  - Curve fitting (time domain filtering).
- Spectral resolution estimation with these two methods.
- Comparison with the theoretical value.

# Optimal filtering: comparison

Expected spectral resolution for this test pixel : 3.785 eV.



Amplitude histogram using **curve fitting**.  $\Delta E_{FWHM} = 3.757 \text{ eV}$ .



Amplitude histogram using **Wiener deconvolution**.  $\Delta E_{FWHM} = 3.465 \text{ eV}$ .

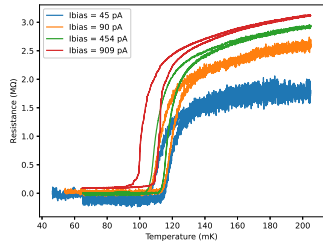
Conclusion : curve fitting and Wiener deconvolution are two efficient optimal filtering methods retrieving the expected theoretical resolution. But difficulties appear when adding sine perturbations or jitters.

# Optimisation of the detector's spectral resolution

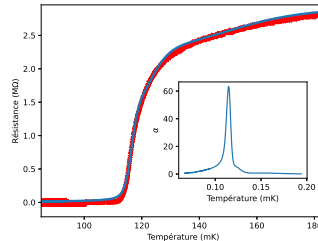
Parameter	Variation	Impact on spectral resolution
Si Volume	↗	↗
Absorber heat capacity	↗	↗
TES NbSi volume (constant resistance)	↗	↘↗
Normal state TES resistance	↗	↘
Heater resistance (constant volume)	↗	→
Heater NbSi volume (constant resistance)	↗	↘↗
Heat-sink temperature	↗	↘
Heat-sink temperature (constant $\Delta T$ )	↗	↘↗
Thermal conductance to heat-sink	↗	↘
Thermal conductance to absorber	↗	↗

Conclusion: spectral resolution at 2.1 eV after optimisations. Comparable to state-of-the-art TESs.

# Characterisation of the new batch of pixels



Superconducting transitions of a 0.5 mm par 0.5 mm with a  $3 \mu\text{m}$ , 13.2 mm meander.  
Suspended by 4 Au wire bondings.

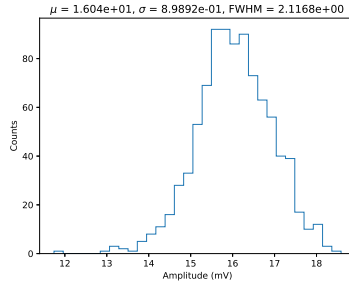


Superconducting transition and curve fitting (exponential) of the 454 pA biasing on the 0.5 mm suspended pixel.

Conclusion: tested pixels present a superconducting transition around the desired temperature (100 mK) with normal state resistances in agreement with requirements. The logarithmic sensitivity is low compared to low impedance TES but higher than doped-Si.

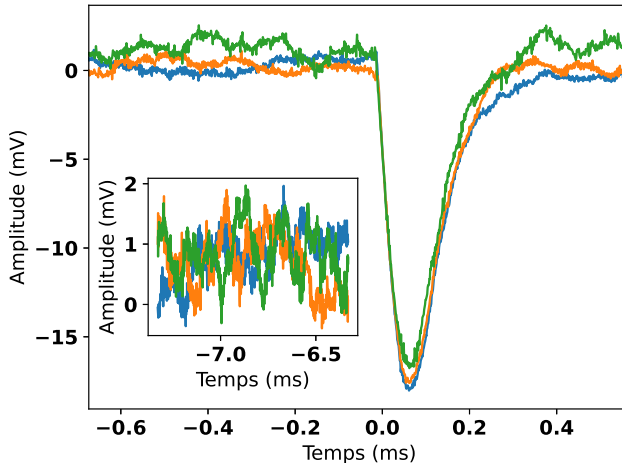
## Amplitude spectra on a 0.5 mm pixel

- Measurements on a small 0.5 mm pixel with **454 pA biasing**.
- Biasing 5x lower because very low critical current  $\Rightarrow$  reduced amplitude.



Amplitude spectrum from  $^{55}\text{Fe}$  X-ray photons.  $\Delta E_{FWHM} = 780 \text{ eV}$ . Biasing current: 454 pA.

Conclusion: coarse resolution: low frequency noise, amplitude 16 mV, expected 28 mV: electronic heat capacity and thermal link to heat sink.  $\Rightarrow$  conception of an improved set-up.

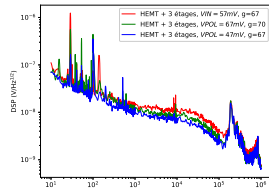


Three pulses from Iron 55 X-rays, 0.5 mmx0.5 mm pixel with 4 gold bondings.

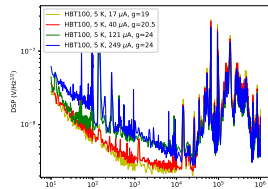
# Noise measurements

Goal: the amplifier's noise should be lower than the expected detector noise, *i.e.* lower than  $1 \text{ nV}/\sqrt{\text{Hz}}$  at 1 kHz.

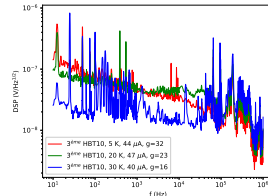
- HEMT and SiGe noise present noise spectra below  $1 \text{ nV}/\sqrt{\text{Hz}}$  at 1 kHz.
- BUT: SiGe noise with emitter degeneracy appears to be higher than expected.
- Multiple tests/measures on SiGe noises at cryogenic temperatures and interpretations.
- HEMT noise not measured (should be below SiGe).



Input noise of HBT100, common emitter at different temperature, same current.

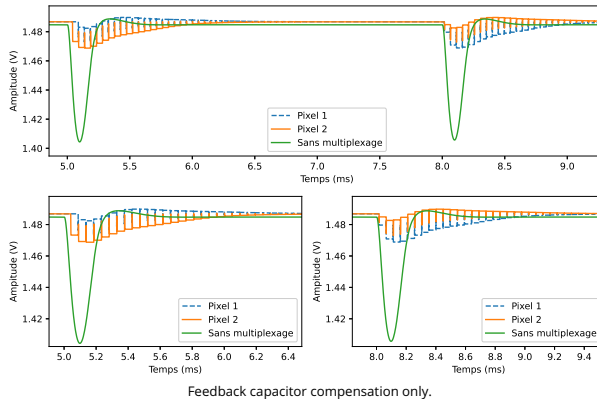


Input noise of HBT100, emitter degeneracy ( $825 \Omega$ ) at 5 K, different current.

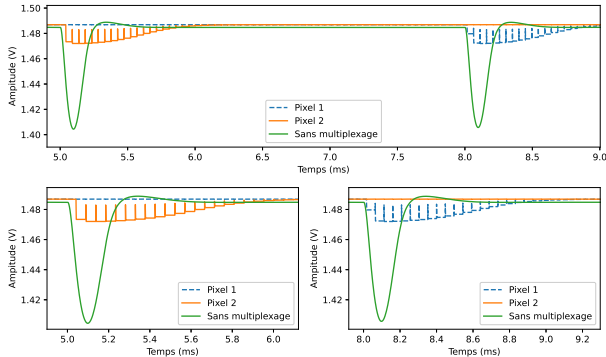


Input noise of last stage HBT10 emitter degeneracy at different temperature, same current.

# First simulations on LTSpice (validation)

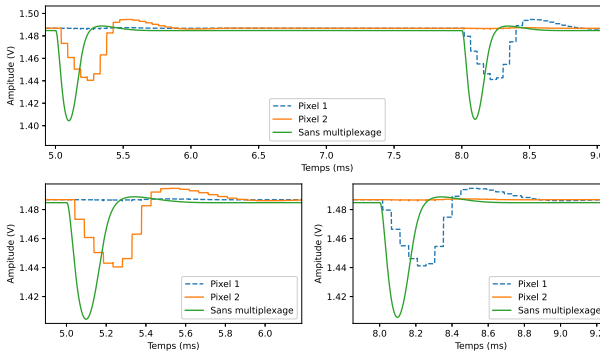


# First simulations on LTSpice (validation)



Feedback capacitor and reset voltage for crosstalk suppression.

# First simulations on LTSpice (validation)

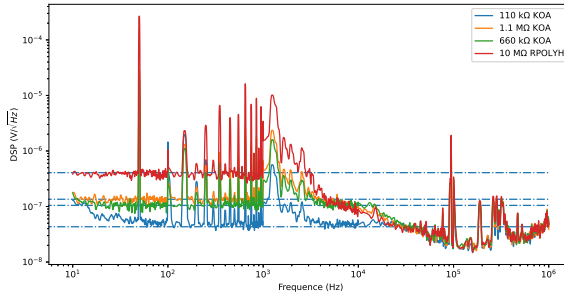


Feedback capacitor, reset voltage and loading of the previous state.

Conclusion: The capacity compensation techniques are working and necessary to retrieve the original amplitude with suppression of crosstalk.

# Noise measurements at room temperature

- Measure the noise of different resistors and of the integrated  $10\text{ M}\Omega$  RPOLYH.
- Validation at room temperature of the set-up between  $50\text{ mK}$  and  $4\text{ K}$  regarding noise pickup.
- Use of a LT6242 for room temperature tests.
- Possible to evaluate the cut-off frequency:  $\sim 35\text{ kHz} \implies C_{in} \sim 41\text{ pF}$ .

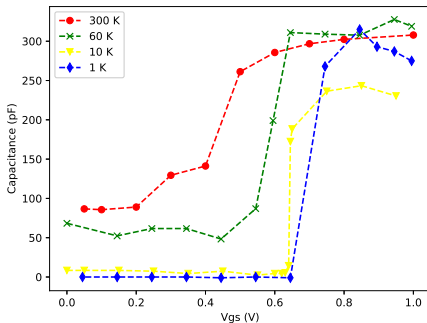


Noise PSD of different resistors passing through the ASIC, the flex and amplified by a room temp. op-amp.

Conclusion: the room temperature noise of the integrated RPOLYH is its Johnson noise. We observe 50 Hz harmonics and a large pic around 1 kHz. We estimate the input capacitance around 40 pF.

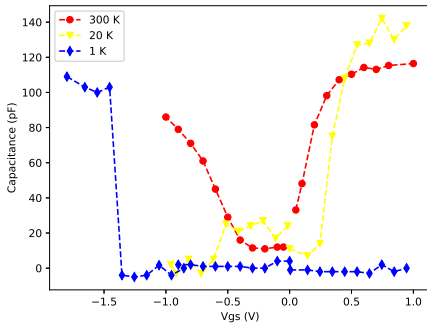
# Determination of the NMOS integrated capacitance value with temperature

- A MOS capacitor is the series connexion of the poly-gate/oxyde/semiconductor capacitance (fixed) and the capacitance of the charges in the depletion/inversion region.
- $C_{max} = C_{ox} = \epsilon_{ox}/l_{ox}$  and  $1/C_{min} = 1/C_{ox} + W_{min}/\epsilon_{sc}$
- Measure only possible for positive voltages (bulk, source and drain grounded).



- NMOS surface : 7 111x90  $\mu\text{m}$  in parallel (selectable)
- Oxyde capacitance roughly constant with T.
- Threshold voltage increasing with decreasing T.
- Expected NMOS capacitance above  $V_{th}$  : 278 pF  $\Rightarrow$  coherent with measurement.
- NMOS capacitance decreasing with T in depletion/inversion region : reaches  $\sim 0$  F at 1 K.

# Determination of the PMOS integrated capacitance value with temperature

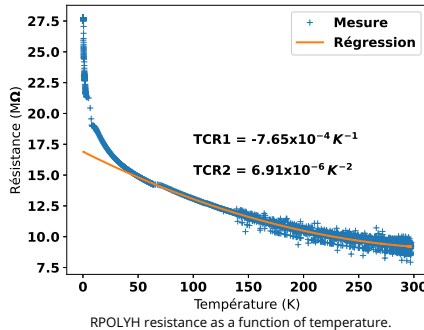


- PMOS surface : 5 192x32  $\mu\text{m}$  in parallel (selectable)
- Oxyde capacitance not determined accurately enough.
- Threshold voltage increasing with decreasing T as well as flatband voltage.
- Expected PMOS capacitance above  $V_{th}$  : 117 pF  $\Rightarrow$  roughly coherent with measurement.
- PMOS capacitance decreasing with T in depletion/inversion region : reaches  $\sim 0$  F at 1 K.
- Maximal capacitance still too small compared to input parasitic  $\Rightarrow$  increase of signal gain.

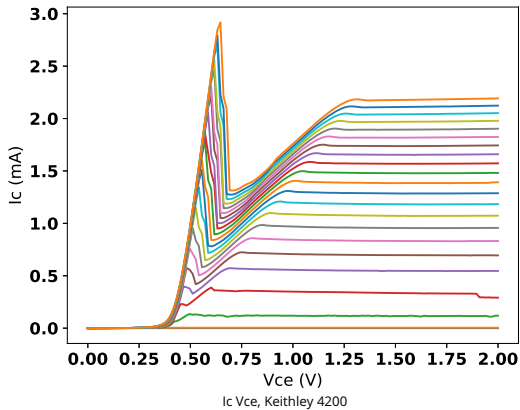
## RPOLYH resistance with temperature.

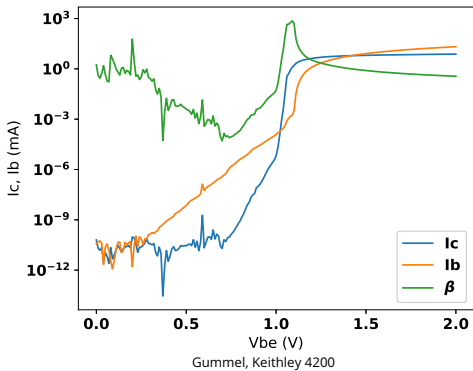
The biasing resistor of the detector is integrated inside each of the 16 channels. No data on low temperature behaviour of this high resistivity poly-Si material  $\Rightarrow$  measurement and calibration needed.

- AMS 2<sup>nd</sup> order polynomial fitting in agreement with measurements down to 70 K.
- Below 70 K: another type of electronic conduction at work. 27 M $\Omega$  at 150 mK.
- Discrepancy between channels below 5%.

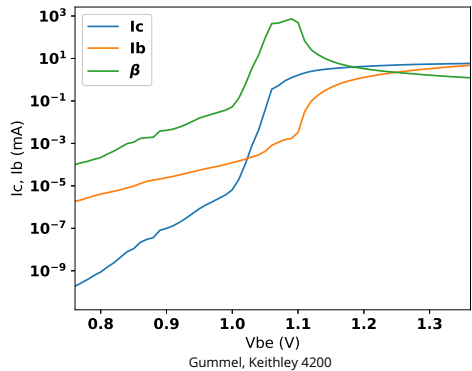


$I_c = f(V_{ce})$  HBT100 650 mK.





Gummel, Keithley 4200



Gummel, Keithley 4200